MACHINING PARAMETER SELECTION BASED ON A COST-BASED OBJECTIVE FUNCTION AND PROCESS STABILITY

Mohammad H. Kurdi, Tony L. Schmitz, and Raphael T. Haftka
Department of Mechanical and Aerospace Engineering
University of Florida
Gainesville, FL, USA

INTRODUCTION

Machining optimization research has enjoyed a rich history. Initial theoretical work by Gilbert in 1950 used the Taylor tool life equation and two criteria, maximum production rate and minimum cost, to determine optimized cutting speed [1]. Subsequent research efforts have applied various optimization criteria, including sums of weighted objectives, and implemented multiple optimization techniques. The purpose of this paper is to demonstrate a single objective function optimization formulation for milling that simultaneously considers tool wear and process dynamics effects in an analytical framework. We compare the costs for optimized conditions and manufacturer-recommended values.

OBJECTIVE SELECTION

A natural candidate for the optimization objective is profit, *P*. Profit may be expressed as:

$$P = \int_{t_0}^{\infty} e^{-rt}(R - C)dt\,, \tag{1}$$

where t_0 is the current time, r is the discount rate that devalues future sales, R is revenue, and C is cost. Revenue is the product of price and the number of components. Cost, however, can have many inputs, which may be categorized into fixed and variable costs. Fixed costs include, for example, building and machinery depreciation, insurance, taxes, interest, indirect labor, engineering, rentals, general supplies, management expenses, and marketing/sales. Examples of variable costs are materials, tooling, labor, utilities/power, and maintenance. Cost considerations specific to machining include, e.g., setup time, part quality, CNC programming, inspection, cycle time, rework, finishing, part handling, fixturing, coolant use and disposal, and tool advance-retract-change times [2].

In job shop situations, the number of units to be sold, x, is typically known once a job is accepted. If we assume that the unit price is also known, then revenue is a fixed value and the objective becomes cost minimization. In the following sections, a method for including both process dynamics and tool wear in a cost minimization formulation is described.

APPROACH

The cost function, $C(x)$, is provided in Eq. 2, where C_f represents fixed costs and C_m is the machining-related cost per part.

$$C(x) = C_f + xC_m \tag{2}$$

We will minimize C_m (Eq. 3) subject to the two constraints shown.

$$\text{Minimize } C_m = t_m r_m + (t_{tch} r_m + C_t)\frac{t_c}{T} \tag{3}$$
$$\text{subject to } b \le b_{lim} \text{ and } \Omega_{min} \le \Omega \le \Omega_{max}$$

Here, t_m is the overall machining time, r_m is the machining cost per unit time, t_{tch} is the tool changing time, C_t is the cost per tool, t_c is the actual cutting time, and T is the tool life. Machining/cutting time and tool life are directly affected by: 1) the selected process parameters, including radial and axial depths of cut, a and b (limited by the process stability as indicated by the first constraint), spindle speed, Ω, and feed per tooth, f_t; and 2) the tool information, including the diameter, d, (which defines the cutting speed, $v = \pi d\Omega$, when combined with the spindle speed), cutting edge geometry, and the number of teeth, N.

The machining time depends on the part path. For simplicity, we define it here as:

$$t_m = L/f, \tag{4}$$

where L is the distance traveled by the tool and f is the feed rate, given by $f = \Omega N f_t$. The tool cutting time can be calculated as:

$$t_c = V/MRR, \quad (5)$$

where V is the volume to be removed and $MRR = abf_t\Omega N$ is the mean material removal rate. The tool changing time, t_{tch}, in Eq. 3 depends on the machining center and can range from less than one second (automated) to several minutes (manual). The machining cost per unit time depends on the manufacturing facility, machining center, and labor costs.

Tool Life Model

Coefficients for tool life models are typically determined from cutting test data. To demonstrate our approach, we have applied the data presented by Tsai *et. al*. [3] for a TiAlN-coated, tungsten carbide endmill (HFK UF440A-4ENSR-D10-R0.5) used to machine SKD61 tool steel. In [3], tool life is represented using an abductive polynomial network. The tool specifications are provided in Table 1 and the cutting conditions are listed in Table 2.

TABLE 1. Tool specifications from Tsai et al. *[3].*

d (mm)	N	Overall length (mm)	Helix angle (deg)	Corner radius (mm)
10	4	100	45	0.5

TABLE 2. Cutting conditions from Tsai et al. *[3].*

v (m/min)	Ω (rpm)	f_t (mm/tooth)	b (mm)	a (mm)
314-628	9994-19989	0.0075-0.15	0.5-1.5	0.5

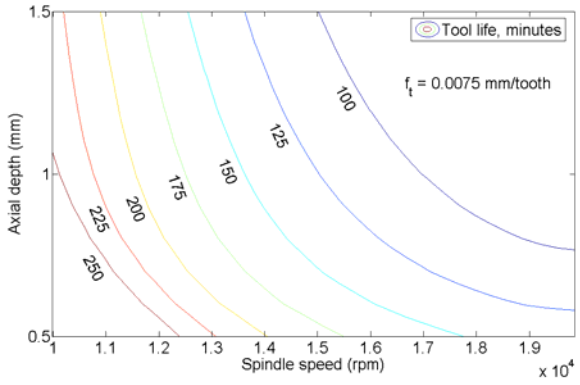

FIGURE 1. Tool life contours from Tsai et al. *[3].*

Tool life contours obtained using the abductive polynomial network for a 0.0075 mm/tooth feed per tooth value (within the Ω and b ranges given in Table 2) are shown in Fig. 1. As expected, the tool life decreases with increasing spindle speed, Ω, and axial depth of cut, b.

For optimization purposes, we wished to extend the allowable operating range beyond the cutting test conditions. Figure 2a shows extrapolated tool life contours for axial depths up to 3.5 mm and spindle speeds down to 2000 rpm. As seen, extrapolation of the abductive polynomial network yields unexpected results; the contours do not follow the general trend of decreased life with increased speed and axial depth. Therefore, we have used the data reported in [3] to generate a Taylor-type tool life model of the general form, $T = Cv^{-p}f_t^{-q}b^{-r}$, where C, p, q, and r are constants. From the 42 tests completed using various v, f_t, and b values, the Taylor-type tool life equation coefficients were determined by least squares fitting:

$$T = 1.9549\text{x}10^6\, v^{-1.6265}\, f_t^{-0.1024}\, b^{-0.2837}, \quad (6)$$

where T is expressed in min, v in m/min, f_t in mm/tooth, and b in mm. In Fig. 2a, it is seen that the Taylor-type model exhibits the expected behavior. Figure 2b shows a comparison between the abductive polynomial network and Taylor-type model over the cutting test range. Reasonable agreement is observed.

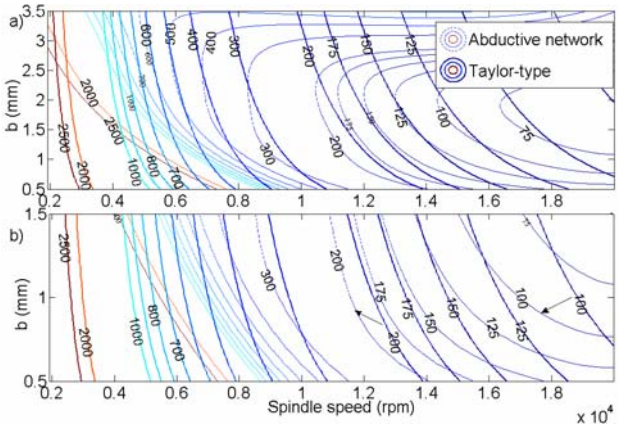

FIGURE 2. Comparison of tool life contours (in minutes) for abductive polynomial network and Taylor-type tool life models (f_t = 0.0075 mm/tooth). a) Extrapolation outside test range – abductive network shows unexpected results. b) Comparison of abductive and Taylor-type tool life models within the test range.

As noted, a key goal of this study was to compare manufacturer-recommended cutting conditions with those determined using the optimization approach. Because manufacturer

recommendations were not available for the tool-workpiece combination used in the Tsai *et al*. study, we selected an equivalent tool from Sandvik Coromant. This enabled us to use their recommended cutting conditions. Sandvik Coromant solid carbide tools with approximately the same coating as the tool in Table 1 have a grade designation GC1630. The SKD61 tool steel machined by Tsai *et al*. corresponds to an ISO CMC No. P03.11 high-alloy steel. The closest available Sandvik Coromant geometry was provided by an R216.34-10045-AC22N tool, p. A148 [4] (see Table 3). Additionally, cutting force coefficients for the ISO CMC No. P03.11 high-alloy steel were given as K_t = 2395x10^6 N/m^2 and K_n = 718x10^6 N/m^2 [4], which proportionally relate the tangential (*t*) and normal (*n*), or radial, direction cutting force components for the rotating cutter to the commanded chip area (i.e., the product of *b* and f_t).

TABLE 3. Sandvik Coromant tool specifications.

d (mm)	*N*	Overall length (mm)	Helix angle (deg)	Corner radius (mm)
10	4	72	45	Chamfer

Tool-Point Frequency Response Function

In order to determine the limiting axial depth of cut as a function of spindle speed (for the first constraint in Eq. 3), the tool point frequency response function (FRF) of the tool-holder-spindle combination must be known. To obtain the tool point FRF, we rigidly coupled models of the selected tool and a CoroGrip precision power chuck (392.410HMD-63 20 077, p. D113 [4]) with a cylindrical collet (393.CGS-20 10 52, p. D165 [4]) to a representative high-speed spindle (FRF determined experimentally) using Receptance Coupling Substructure Analysis [5-7]. Figure 3 shows the predicted assembly FRF as reflected at the tool point.

Process Stability Model

We applied the frequency domain approach given in [8] to predict the limiting axial depth of cut as a function of spindle speed. Inputs to the algorithm include the tool point FRF, cutting force coefficients, and radial depth of cut. Using the Fig. 3 FRF, K_t = 2395x10^6 N/m^2 and K_n = 718x10^6 N/m^2 cutting force coefficients [4], and *a* = *d*, the stability lobe diagram shown in Fig. 4 was obtained, where *b*-Ω combinations below the stability boundary indicate stable, or chatter-free, cutting.

RESULTS

We considered cost minimization for removing a cube of material with dimension *W* = 100 mm. For the full radial immersion conditions (*a* = *d*) shown in Fig. 5, the distance traveled by the tool is:

$$L = \frac{W}{b}\left(\frac{2W}{a}(W+d)+W\right). \qquad (7)$$

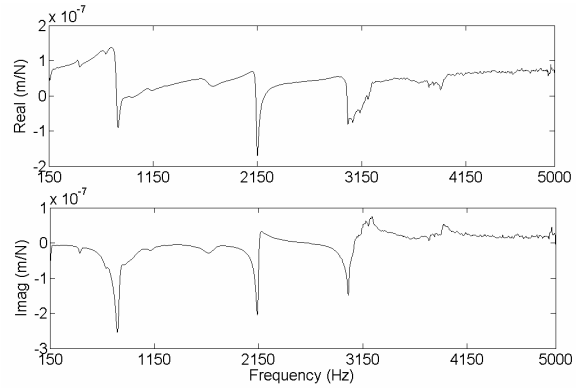

FIGURE 3. Tool point FRF for selected tool-holder-spindle combination.

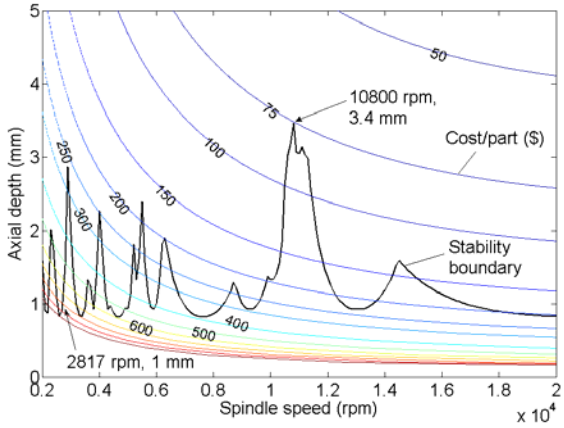

FIGURE 4. Stability lobe diagram for test case. Cost per part contours are also shown (f_t = 0.027 mm/tooth).

Based on the cost parameters listed in Table 4 and travel distance defined by Eq. 7, the cost per part was determined as a function of axial depth, *b*, and spindle speed, Ω (see contours in Fig. 4). It is seen that the minimum cost for chatter-free cutting corresponds to the highest possible combination of *b* and Ω defined by the stability boundary (3.4 mm and 10800 rpm). A gradient-based search algorithm with multiple guesses was implemented in Matlab (to handle

discontinuities in the stability boundary) and verified this operating point.

TABLE 4. Cost parameters for test case.

t_{tch} (sec)	C_t ($/tool)	r_m ($/min)
4	114	1

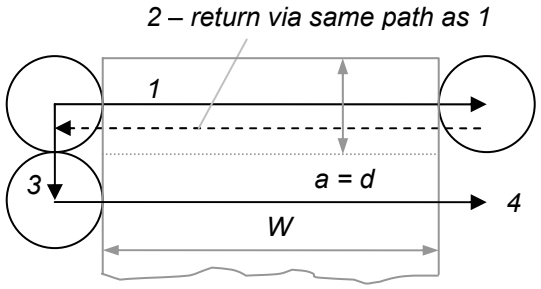

FIGURE 5. Part path for machining cube of dimension W = 100 mm. This path (1, 2, 3, 4, …) is repeated in multiple axial levels as required by the limiting axial depth of cut.

The manufacturer-recommended cutting conditions for the selected tool-workpiece combination (p. A303, [4]) are listed in Table 5, where a correction factor of 1.18 was applied to obtain the recommended spindle speed corresponding to the SKD61 material hardness (p. A321, [4]). In a previous publication of the Sandvik Coromant handbook [9], the recommended axial depth for a slotting operation was listed as 50% of the tool diameter. This would correspond to b = 5 mm, which is in the unstable region for our test case.

TABLE 5. Manufacturer-recommended cutting conditions.

v (m/min)	f_t (mm/tooth)	Ω (rpm)	Depth (mm)
88.5	0.027	2817	$a \times b > d$

For the conditions listed in Table 5, if a stable depth of cut of 1 mm is selected (see Fig. 4 at 2817 rpm), the associated cost per part for machining the ISO CMC No. P03.11 high-alloy steel 100 mm cube is $775.44. If the optimized parameters are selected (10800 rpm, b = 3.4 mm), the cost is $76.78 – a 90% reduction. See Table 6. Even if a more conservative axial depth of 2.5 mm is used (to move away from the stability boundary), a cost reduction of 87% is still achieved. This simple example demonstrates the importance of considering the process dynamics, in addition to tool wear, for machining parameter selection.

TABLE 6. Cost comparison – the optimized conditions provide a 90% cost reduction.

Source	b (mm)	Ω (rpm)	C_m ($)
Sandvik	1.0	2817	775.44
Optimized	3.4	10800	76.78

CONCLUSIONS

In this paper we formulated a cost-based objective function which considered both tool life and process stability. Based on test data from the literature, it was shown that significant cost reduction relative to manufacturer recommendations could be achieved through the application of dynamic models within an optimization framework.

ACKNOWLEGEMENTS

This work was supported by the National Science Foundation (DMI-0238019), the Office of Naval Research (Young Investigator program), TechSolve, and the Naval Surface Warfare Center-Carderock Division. The authors also wish to thank G. Hazelrigg for many helpful discussions.

REFERENCES

1. Gilbert, W., 1950, Economics of Machining, *Machining – Theory and Practice*, American Society for Metals, Metals Park, OH, 465-485.
2. Stephenson, D. and Agapiou, J., 1997, Metal Cutting Theory and Practice, Marcel Dekker, Inc., New York, NY.
3. Tsai, M. K., Lee, B. Y., and Yu, S. F., 2005, A Predicted Modeling of Tool Life of High Speed Milling for SKD61 Tool Steel, *International Journal of Advanced Manufacturing Technology*, 26: 711.
4. Rotating Tools and Inserts Handbook, Sandvik Coromant, LIT-CAT 04-R.
5. Schmitz, T. and Donaldson, R., 2000, Predicting High-Speed Machining Dynamics by Substructure Analysis, *Annals of the CIRP*, 49/1: 303-308.
6. Schmitz, T., Davies, M., and Kennedy, M., 2001, Tool Point Frequency Response Prediction for High-Speed Machining by RCSA, *Journal of Manufacturing Science and Engineering*, 123: 700-707.
7. Schmitz, T. and Duncan, G.S., 2005, Three-Component Receptance Coupling Substructure Analysis for Tool Point Dynamics Prediction, *Journal of Manufacturing Science and Engineering*, 127/4: 781-790.
8. Altintas, Y. and Budak, E., 1995, Analytical Prediction of Stability Lobes in Milling, *Annals of the CIRP*, 44/1: 357.
9. Rotating Tools and Inserts Handbook, Sandvik Coromant, LIT-CAT 01-R.